Bull Earthquake Eng (2017) 15:1019–1035
DOI 10.1007/s10518-016-9983-7

ORIGINAL RESEARCH PAPER

Filtering effect induced by rigid massless embedded foundations

Riccardo Conti[1] · **Marco Morigi**[2] · **Giulia M. B. Viggiani**[2]

Received: 23 March 2016 / Accepted: 2 August 2016 / Published online: 10 August 2016

Abstract It is well recognised that the dynamic interaction between structure, foundation and supporting soil can affect significantly the seismic behaviour of buildings. Among other effects, embedded and deep foundations can filter the seismic excitation, causing the foundation input motion (FIM) to differ substantially from the free-field motion. This paper presents a theoretical and numerical investigation on the filtering effect induced by rigid massless embedded foundations. Based on the results of dimensional analysis and numerical simulations, it is shown that the problem can be reasonably described by two sole dimensionless groups, namely: (1) $\omega H/V_S$, relating the wave length of the signal to the embedment depth of the foundation, and (2) the aspect ratio of the foundation, B/H, where B is the foundation width in the polarization plane. New simplified and physically sound expressions are derived for the kinematic interaction factors, $I_u = u_{FIM}/u_{ff0}$ and $I_\theta = \theta_{FIM}H/u_{ff0}$, which are frequency-dependent transfer functions relating the harmonic steady-state motion experienced by the foundation to the amplitude of the corresponding free-field surface motion. Standard methods for using these functions in the evaluation of the FIM are critically reviewed, with reference to both static and dynamic procedures for the seismic design of structures.

Keywords Soil–structure interaction · Foundation input motion · Free-field motion · Kinematic response · Embedded foundation

✉ Riccardo Conti
riccardo.conti@unicusano.it

Marco Morigi
marco.morigi@uniroma2.it

Giulia M. B. Viggiani
viggiani@uniroma2.it

[1] Università di Roma Niccolò Cusano, Via Don Carlo Gnocchi, 3, 00166 Rome, Italy

[2] DICII, Università di Roma Tor Vergata, Rome, Italy

1 Introduction

The seismic performance of structures is usually evaluated under a fixed-base assumption by applying a base slab input motion equal to the free-field motion, i.e. neglecting the dynamic interaction between the structure, the foundation and the supporting soil soil–structure interaction (SSI). Nevertheless, the presence of a deformable soil–foundation system affects the dynamic behaviour of buildings in at least three different ways, making the seismic response of the flexibly-supported structure possibly different from that of the rigidly-supported counterpart (Bielak 1975; Mylonakis and Gazetas 2000): (1) it lengthens the fundamental period of the structure; (2) it allows additional dissipation of energy into the soil by radiation and hysteresis; (3) it filters the signal transmitted to the structure by incident waves, as a results of both base slab averaging (Veletsos et al. 1997) and embedment effects (Elsabee and Morray 1977).

SSI can be thought conveniently, both from a conceptual and computational point of view, as the contribution of two concurrent phenomena (Mylonakis et al. 2006): (1) kinematic interaction, in which a massless foundation modifies the motion of the surrounding soil by means of its sole stiffness and (2) inertial interaction, in which the motion of the foundation itself is further modified by the D'Alembert forces acting in the structure-foundation system. The distinction between kinematic and inertial effects, which also underlies the substructure method, provides a powerful key to interpretation of SSI problems, as observed in experimental works (Rayhani and El Naggar 2008), numerical works (Mahsuli and Ghannad 2009; Politopoulos 2010; Vega et al. 2013) and field measurements (Stewart 2000; Kim and Stewart 2003), where many factors can affect the overall dynamic response of the structure.

By focusing on the filtering effect, kinematic interaction has been recognised to play a significant role in the case of both embedded (Avilés et al. 2002; Politopoulos 2010) and deep foundations (Di Laora and de Sanctis 2013), for which the foundation input motion (FIM) can differ substantially from the free-field motion recorded at ground surface. Under the assumption of vertically propagating plane shear waves, base slab averaging cannot occur and filtering effect is physically related to the inability of the foundation elements to follow soil deformations induced by travelling waves.

In the case of rigid embedded foundations, scattering effects reduce the horizontal displacement of the base slab, u_{FIM}, with respect to the free-field case, u_{ff0}, but can introduce a rotational component, θ_{FIM}. This phenomenon can be described by two kinematic response factors, namely $I_u = u_{\mathrm{FIM}}/u_{\mathrm{ff0}}$ and $I_\theta = \theta_{\mathrm{FIM}} H/u_{\mathrm{ff0}}$, which are frequency-dependent transfer functions relating the harmonic steady-state motion experienced by the foundation to the amplitude of the corresponding free-field surface motion (see Fig. 1).

Many works in the literature have been devoted to the problem of filtering effects induced by rigid embedded foundations, using different numerical techniques, most of them considering the case of a massless rigid foundation—with cylindrical or rectangular shape—embedded in a uniform elastic or viscoelastic half-space (Elsabee and Morray 1977; Day 1978; Dominguez 1978; Karabalis and Beskos 1986; Luco and Wong 1987; Mita and Luco 1989). More recently, Brandenberg et al. (2015) have proposed a Winkler-type simplified model, relating the kinematic response factors to the translational and rotational impendence functions for the soil.

Further studies, taking into account both the soil–foundation system and the superstructure (complete SSI), have shown that the filtering effect is usually beneficial for squat

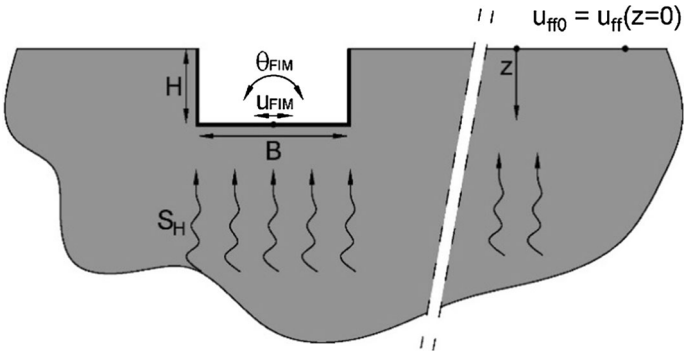

Fig. 1 Schematic representation of the soil–foundation kinematic interaction in the case of embedded foundations and vertically propagating SH waves

structures while it may increase the ductility demand in the case of slender buildings with deeply embedded foundations or basements (Mahsuli and Ghannad 2009). Moreover, in the case of base isolated structures, such as nuclear plants, where standard devices have isolation capacity only in the horizontal plane, the dynamic response of non-isolated modes can be significantly amplified by rocking oscillations of the foundation (Politopoulos 2010; Politopoulos et al. 2015).

The filtering effect induced by embedded foundations is usually described using the formulas proposed by Elsabee and Morray (1977):

$$I_u = \frac{u_{FIM}}{u_{ff0}} = \begin{cases} \cos\left(\dfrac{\omega H}{V_S}\right) & \omega \le 0.7\dfrac{\pi}{2}\dfrac{V_S}{H} \\ 0.453 & \omega > 0.7\dfrac{\pi}{2}\dfrac{V_S}{H} \end{cases} \tag{1}$$

$$I_\theta = \frac{\theta_{FIM} \cdot H}{u_{ff0}} = \begin{cases} \dfrac{2H}{B}0.257\left[1 - \cos\left(\dfrac{\omega H}{V_S}\right)\right] & \omega \le \dfrac{\pi}{2}\dfrac{V_S}{H} \\ \dfrac{2H}{B}0.257 & \omega > \dfrac{\pi}{2}\dfrac{V_S}{H} \end{cases} \tag{2}$$

where B is the foundation width, ω is the angular frequency of the excitation and V_S is the shear wave velocity of the supporting soil (FEMA 440 2005; Mylonakis et al. 2006).

As shown in Fig. 2, despite their simplicity these equations provide a quite crude approximation of the actual physical phenomenon, essentially relating the motion of the rigid foundation to the translation of the free-field at the foundation level [Eq. (1)] and to the so-called free-field "pseudo-rotation", resulting from the differential displacement of the soil in the embedment region [Eq. (2)].

This paper presents a numerical and theoretical investigation of the filtering effect induced by rigid massless embedded foundations. The goal of this study is threefold: (1) to offer insight into the relevant factors affecting the problem; (2) to extend the numerical observations available in the literature; (3) to define new simplified, but physically sound, solutions to be incorporated in recommendations for the seismic design of structures with embedded foundations. Results of this work will be useful not only to improve the understanding of the mechanisms underlying filtering effects, such as the little relevance of the three-dimensional features of the foundation, but also for the design practice.

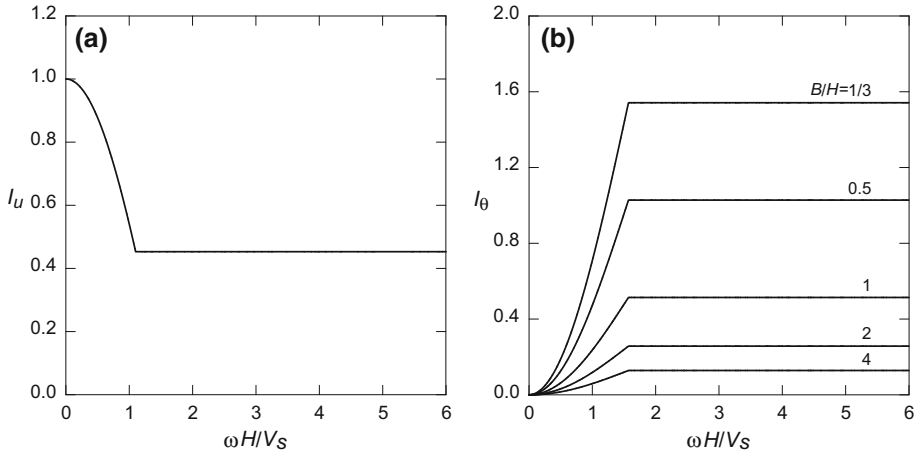

Fig. 2 Formulas proposed by Elsabee and Morray (1977) for the kinematic response factors: **a** I_u and **b** I_θ

2 Problem definition and dimensional analysis

In this section we derive the dimensionless groups governing the filtering effect induced by embedded foundations, under the assumption of vertically propagating plane shear waves. We refer to the general case of a rectangular foundation (embedment depth H, width B, length L, mass density ρ^*, shear modulus G^*, damping ratio ξ) embedded in a homogeneous isotropic visco-elastic soil layer (depth H_d, mass density ρ, shear modulus G, Poisson's ratio ν, damping ratio ξ). Table 1 summarises the 14 physical variables relevant for the problem at hand, which can be formulated as:

Table 1 Variables governing the dynamic interaction between soil and embedded foundations

	Variable	Dim.	Description
Foundation input motion	u_{FIM}	L	Base horizontal disp.
	θ_{FIM}	L^0	Rotation
Free-field motion	u_{ff0}	L	Surface horizontal disp.
	ω	T^{-1}	Angular frequency
Foundation properties	ρ^*	ML^{-3}	Mass density
	G^*	$MT^{-2}L^{-1}$	Shear modulus
	H	L	Embedment
	B	L	Width
	L	L	Length
Soil properties	ρ	ML^{-3}	Mass density
	G	$MT^{-2}L^{-1}$	Shear modulus
	ν	L^0	Poisson's ratio
	ξ	L^0	Damping ratio
	H_d	L	Depth of soil deposit

$$\begin{aligned} u_{FIM} &= f\left(u_{ff0}, \omega, H, B, L, \rho^*, G^*, \rho, G, \xi, \nu, H_d\right) \\ \theta_{FIM} &= g\left(u_{ff0}, \omega, H, B, L, \rho^*, G^*, \rho, G, \xi, \nu, H_d\right) \end{aligned} \tag{3}$$

Applying the Buckingham theorem, it is possible to rescale Eq. (3) in dimensionless form, using H, G and ρ as dimensionally independent variables:

$$\begin{aligned} I_u &:= \frac{u_{FIM}}{u_{ff0}} = F\left(\frac{\omega H}{V_S}, \frac{\rho^*}{\rho}, \frac{G^*}{G}, \frac{B}{H}, \frac{L}{H}, \frac{H_d}{H}, \xi, \nu\right) \\ I_\theta &:= \frac{\theta_{FIM} H}{u_{ff0}} = G\left(\frac{\omega H}{V_S}, \frac{\rho^*}{\rho}, \frac{G^*}{G}, \frac{B}{H}, \frac{L}{H}, \frac{H_d}{H}, \xi, \nu\right) \end{aligned} \tag{4}$$

The dimensionless ratios in Eq. (4) take into account the physical, mechanical and geometrical properties of the problem. Among these,

1. $\omega H/V_S$ relates the embedment depth of the foundation to the wavelength of the excitation ($\lambda = V_S/f = 2\pi V_S/\omega$), i.e. the deeper the foundation the longer the wavelengths which can be filtered by scattering effects;
2. G^*/G and ρ^*/ρ are the relative shear stiffness and mass density, respectively, between the foundation and the soil: the stiffer and the denser the foundation, the stronger its filtering capacity;
3. H_d/H is the relative depth between the soil deposit and the foundation embedment, which, for soil layers of finite depth, can introduce spurious oscillations in the kinematic interaction factors (Elsabee and Morray 1977);

In order to reduce the problem at hand and/or in the light of a kinematic-inertial decomposition method, some simplifying assumptions are usually introduced in the literature, i.e.: the embedded foundation is rigid ($G^*/G \gg 1$) and massless ($\rho^*/\rho \ll 1$); the soil deposit is assimilated to a homogeneous half-space ($H_d/H \gg 1$). As far as ξ and ν are concerned, numerical works have shown that, while affecting the dynamic response of both the foundation and the soil, they have a minor influence on the kinematic response factors (Mita and Luco 1989; Di Laora and de Sanctis 2013). Moreover, it will be shown in the following that, as far as the aspect ratios of the foundation are concerned, only the foundation width B in the polarization plane of the shear wave affects significantly the filtering phenomenon. Under these assumptions, the interaction factors can be expressed as functions of two sole parameters:

$$\begin{aligned} I_u &= F\left(\frac{\omega H}{V_S}, \frac{B}{H}\right) \\ I_\theta &= G\left(\frac{\omega H}{V_S}, \frac{B}{H}\right) \end{aligned} \tag{5}$$

By introducing a further hypothesis on the foundation geometry, two limiting 1D conditions can be identified, i.e.:

1. $B/H = 0$ (infinitely thin foundation): the difference between the FIM and the corresponding free-field surface motion is related only to the variation of ground motion with depth. As a consequence, the two kinematic interaction factors can be computed with reference to the free-field motion in the embedment region, assuming elastic behaviour for the soil ($\xi = 0$), as:

$$I_u|_{(B/H=0)} = \frac{u_{ff}|_{z=H}}{u_{ff0}} = \cos\left(\frac{\omega H}{V_S}\right)$$
$$I_\theta|_{(B/H=0)} = \frac{\theta_{ff} \cdot H}{u_{ff0}} = 1 - \cos\left(\frac{\omega H}{V_S}\right) \quad (6)$$

where $\theta_{ff} = \left(u_{ff0} - u_{ff}|_{z=H}\right)/H$ is the free-field pseudo-rotation of the soil.

2. $B/H = \infty$ (infinitely extended foundation): the foundation cannot rotate ($\theta_{FIM} = 0$) and the half-space condition results in $u_{FIM} = u_{ff0}$. As a consequence, the two kinematic interaction factors reduce to:

$$I_u|_{(B/H=\infty)} = 1$$
$$I_\theta|_{(B/H=\infty)} = 0 \quad (7)$$

These asymptotic conditions will be used in the following both to interpret numerical results and to provide simplified solutions for design.

3 Numerical analyses

A total of 17 plane-strain analyses of a rectangular foundation of width B and depth H, embedded in an homogeneous half-space, were carried out in the time domain using the finite difference code FLAC 2D v7 (Itasca 2011). Moreover, two three-dimensional analyses were carried out with the code FLAC 3D. The complete set of analyses is reported in Table 2, with the ratio B/H ranging from 0.25 to 20.

Table 2 Summary of the numerical analyses

#	H (m)	B (m)	B/H	L/B	B_m (m)	H_m (m)
1	12	3	0.25	∞	300	27
2	12	6	0.5	∞	300	27
3	3	3	1	∞	300	27
4	6	6	1	∞	300	27
5	12	12	1	∞	300	27
6	3	6	2	∞	300	27
7	6	12	2	∞	300	27
8	12	24	2	∞	300	27
9	3	12	4	∞	300	27
10	6	24	4	∞	300	27
11	12	48	4	∞	450	27
12	3	18	6	∞	300	27
13	6	36	6	∞	450	27
14	12	72	6	∞	450	27
15	3	30	10	∞	450	27
16	6	60	10	∞	450	27
17	3	60	20	∞	450	27
18	6	6	1	1	100	27
19	6	12	2	1	100	27

3.1 Model definition

Figure 3 shows the typical mesh adopted in this study. The soil was modelled as a linear visco-elastic isotropic material, with mass density $\rho = 1.835$ t/m^3, shear wave velocity $V_S = 100$ m/s and Poisson ratio $v = 0.3$. A Rayleigh viscous damping was used, with a given value of 2 % at the reference frequencies of 1 and 10 Hz.

The rigid massless foundation was modelled as an open excavation with rigid boundaries and supports, in order to enforce rigid body displacements. To this purpose, elastic beams with reduced mass density were introduced (E = 5.0 GPa, A = 7.0 m^2, I = 6.0 m^4, $\rho_b = 0.008$ t/m^3), both along the boundaries of the foundation and as an internal frame, thus increasing the overall shear stiffness of the foundation without affecting significantly its total mass. Perfect contact was assumed between the sidewalls and the soil elements.

Free-field boundary conditions were applied along the lateral sides of the mesh, involving the coupling of the main grid with a one-dimensional free-field column through viscous dashpots, in such a way that outward waves originating from the interior of the model can be properly absorbed.

As far as the boundary condition at the base of the mesh is concerned, both viscous dashpots and the dynamic input were applied in order to reproduce the upward propagation of shear waves within a semi-infinite domain (Joyner and Chen 1975). The input was a constant amplitude sinusoidal sweep, defined in terms of a horizontal displacement time history, with a duration of 60 s and a frequency increasing linearly with time from 0.5 to 10 Hz (Fig. 4). This range was chosen to include the typical frequency content of real earthquakes.

The dimensions of the mesh were chosen after a preliminary parametric study so as to minimise possible side effects due to spurious wave reflections at boundaries, and hence to recover free field conditions. The elements of the mesh have a maximum size of 0.75 m close to the foundation, in order to describe correctly the minimum wavelength of the applied signal ($\lambda_{min} = V_S/f_{max} = 10$ m).

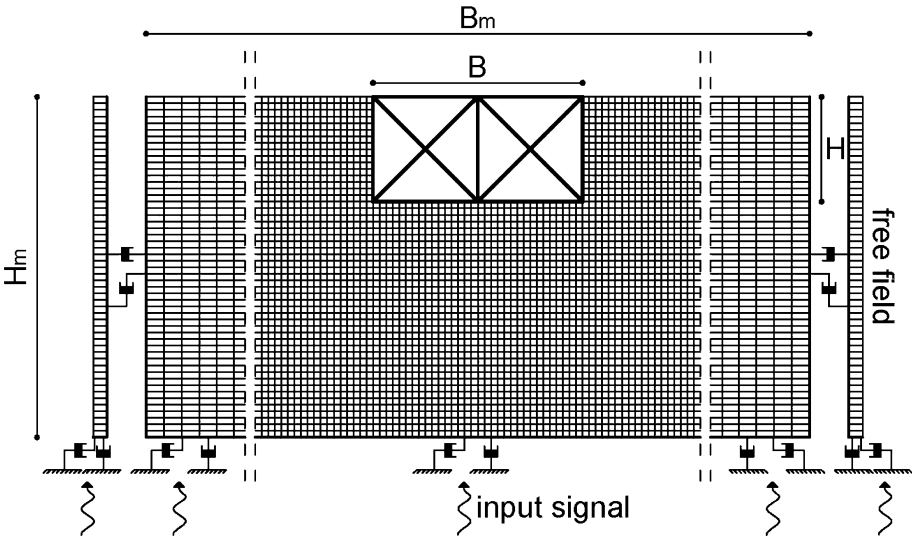

Fig. 3 2D analyses: finite difference model

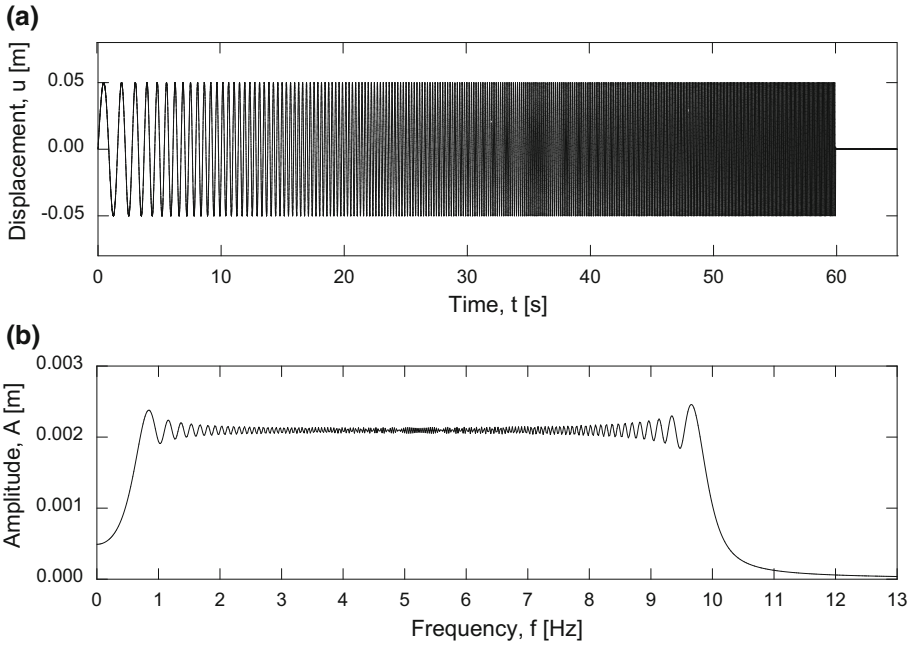

Fig. 4 Sweep input signal: **a** displacement time history and **b** Fourier amplitude spectrum

Moving to 3D analyses, the square foundation ($B/L = 1$) was modelled as an empty excavation, with shell elements of increased stiffness and reduced mass density attached to the internal boundaries. The numerical model is consistent with that adopted in the 2D analyses, in terms of boundary conditions, dynamic input, mesh discretisation, and mechanical properties of both soil and foundation elements.

4 Results

The complex valued functions I_u and I_θ were obtained from the Fourier transform of $u_{\mathrm{ff0}}(t)$, $u_{\mathrm{FIM}}(t)$ and $\theta_{\mathrm{FIM}}(t)$, where u_{FIM} corresponds to the horizontal displacement of the bottom centre of the foundation and θ_{FIM} is computed as $(v_1–v_2)/B$, where v_1 and v_2 are the vertical displacements of the two corners at the base of the foundation. As an example, Fig. 5 shows, for analysis No. 11, the numerical values of the real part, imaginary part and amplitude of (a) I_u and (b) I_θ.

In order to ascertain three-dimensional effects on the filtering problem, Fig. 6 compares the results from this study ($B/H = 1$, 2 and $L/B = 1$, ∞), in terms of (a) $|I_u|$ and (b) $|I_\theta|$, with some of those available in the literature, obtained with BEM, FEM or hybrid BEM–FEM approaches. All literature results refer to the case of cylindrical (Day 1978; Luco and Wong 1987) and square (Mita and Luco 1989) foundations ($L/B = 1$) embedded in a uniform elastic half-space, with the only exception of Elsabee and Morray (1977), who considered a cylindrical foundation embedded in an elastic soil layer of finite depth overlying a rigid bedrock. In spite of showing some scatter, numerical data are in substantial agreement, both qualitatively and quantitatively, with a maximum difference of

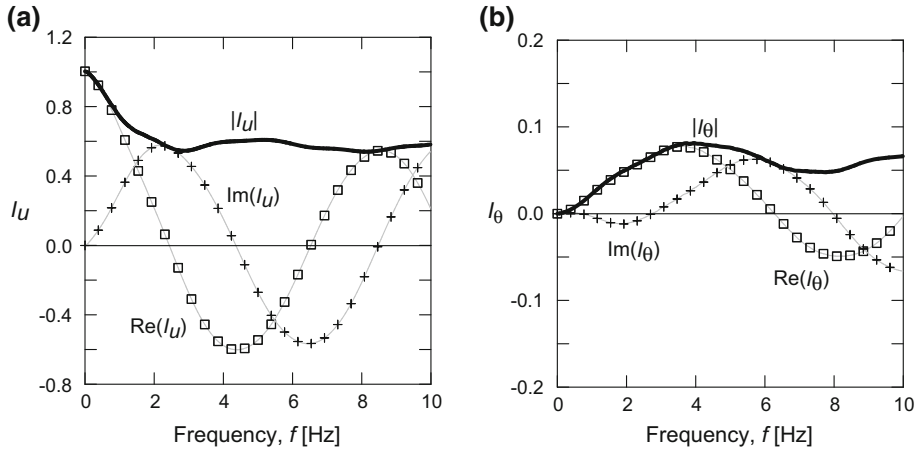

Fig. 5 Analysis No. 11: real and imaginary part of the kinematic interaction factors: **a** I_u and **b** I_θ

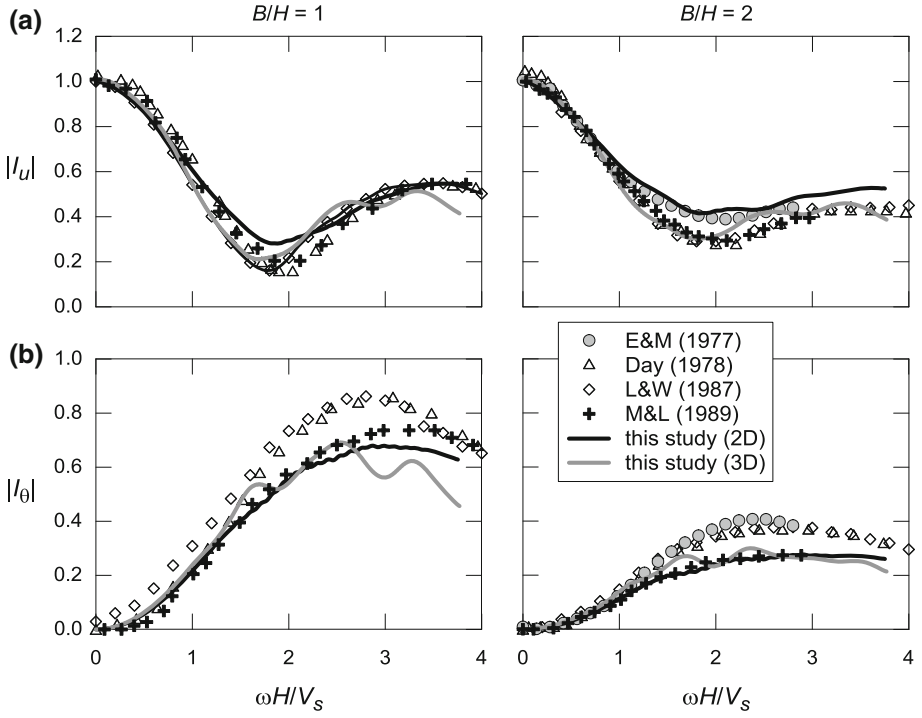

Fig. 6 Comparison between numerical FDM results ($B/H = 1, 2$) and literature data, in terms of: **a** $|I_u|$ and **b** $|I_\theta|$

±15 % on the average in terms of I_θ ($B/H = 2$). Moreover, FDM results are in perfect agreement with each other and with those reported by Mita and Luco (1989). Based on this comparison, it is apparent that the ratio L/H has a minor influence on the kinematic interaction factors, with respect to $\omega H/V_S$ and B/H, and, therefore, that it can be ignored

without any loss of relevant information. This implies that, when looking at filtering effects, 2D analyses provide a reasonable representation of the 3D behaviour of rigid embedded foundations.

Figure 7 shows the numerical values of (a) $|I_u|$ and (b) $|I_\theta|$, as a function of the dimensionless frequency $\omega H/V_S$ and for different values of B/H, together with the theoretical solutions for the 1D limit conditions of $B/H = 0$ and $B/H = \infty$. For small B/H (squat/slender foundations), the interaction factors tend to the free-field 1D conditions, where filtering effects are mostly due to the embedment of base slab. In this condition, $|I_u|$ shows an oscillating trend, with local minima and maxima clearly related to the resonant frequencies of the corresponding free-field case, and a significant rocking component emerges in the FIM, as reflected by $|I_\theta|$. On the other hand, for large B/H values (spread foundations), both factors tend to stabilize, moving towards the asymptotic solution for $B/H = \infty$, without significant oscillations as $\omega H/V_S$ increases. As a result, filtering of the horizontal displacements reduces, but no rocking component is introduced. In other words, numerical analyses indicate that both I_u and I_θ are strongly affected by the aspect ratio of the foundation and are not related merely to the embedment depth of the foundation. In particular, for a given value of H, the larger the foundation the smaller the overall filtering effect induced on the free-field ground motion.

Based on the best fit of numerical data, simplified expressions for $|I_u|$ and $|I_\theta|$ were defined using ad hoc functions which allow to recover the 1D limiting conditions as $B/H \to 0$ or $B/H \to \infty$:

$$\left|I_u\left(\frac{\omega H}{v_s},\frac{B}{H}\right)\right| = a_1\frac{1+a_2\left(\frac{\omega H}{v_s}\right)^2}{1+\left(\frac{\omega H}{v_s}\right)^2} + (1-a_1)\frac{\left|\cos\left(a_3\frac{\omega H}{v_s}\right)\right|}{\left[1+\left(\frac{\omega H}{v_s}\right)^2\right]^{2a_1}} \tag{8}$$

$$\left|I_\theta\left(\frac{\omega H}{v_s},\frac{B}{H}\right)\right| = a_4\left[1-\cos\left(\frac{\omega H}{v_s}\right)\right] \tag{9}$$

in which coefficients a_1, a_2, a_3, a_4 depend on the ratio B/H, as detailed in "Appendix". As shown in Fig. 8, Eqs. (8) and (9) provide a good description of the actual trend exhibited

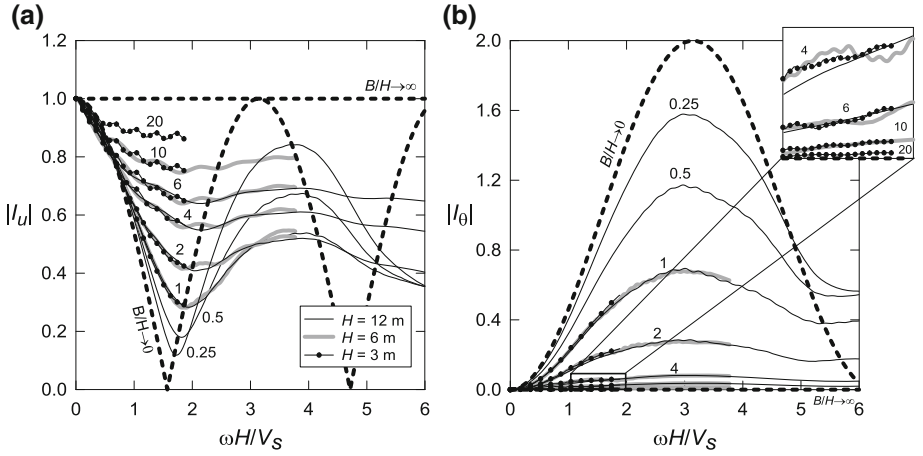

Fig. 7 Numerical results and limit conditions of: **a** $|I_u|$ and **b** $|I_\theta|$

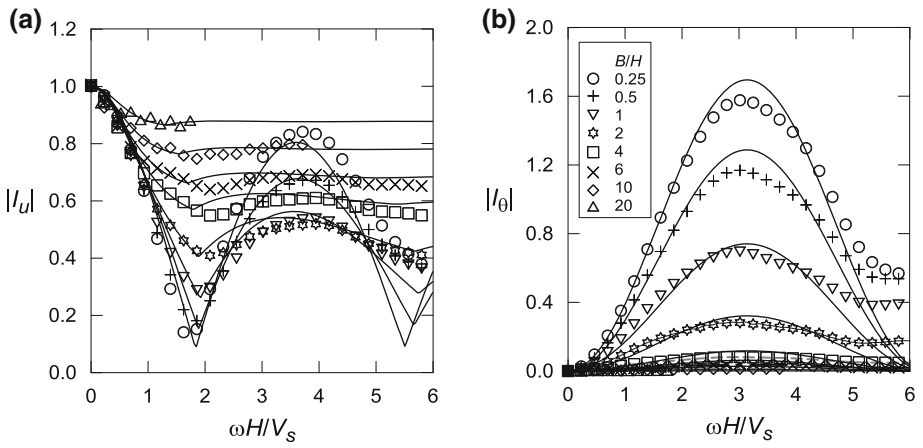

Fig. 8 Comparison between numerical results (*symbols*) and interpolating functions (*lines*): **a** $|I_u|$ and **b** $|I_\theta|$

by $|I_u|$ and $|I_\theta|$, particularly for $\omega H/V_S < 5$, which corresponds to the range of frequencies typical of real earthquakes.

5 Guidelines for design

In the light of the results presented so far, and bearing in mind that the accuracy of any simplified method should be consistent with the uncertainties involved in the characterization of the free-field ground motion, this section aims to review critically standard guidelines for including filtering effects in the evaluation of the FIM (FEMA 440 2005; Mylonakis et al. 2006). We will refer to both dynamic and static procedures for the seismic design of structures, where the design earthquake is defined in terms of a time history or a response spectrum, respectively.

Since the interaction factors are complex valued transfer functions, the mathematical rigorous procedure for computing the FIM consists in applying I_u and I_θ to the Fourier spectrum of the free-field motion, when the latter is defined as a time history (Method M1). However, taking into account that simplified formulas are available only for real-valued functions $|I_u|$ and $|I_\theta|$, the latter are adopted in the design practice, ignoring any possible phase shift between the translation and rocking components of the foundation motion (Method M2).

Moving to static procedures, Mylonakis et al. (2006) suggested to apply $|I_u|$ and $|I_\theta|$ directly to the free-field acceleration spectrum ($S_{a,ff0}(\omega)$), if the design earthquake is specified in this form (Method M3). Accordingly, for a structural mass located at a vertical distance H_c from the base, foundation rocking and translation result in:

$$S_{a,FIM}(\omega) = [|I_u(\omega)| + |I_\theta(\omega)| \cdot H_c/H] S_{a,ff0}(\omega). \tag{10}$$

Clearly, methods M2 and M3 involve quite crude simplifications, whose effects must be ascertained. To this end, we considered the ideal case of an embedded foundation ($H = 6$ m, $B/H = 1$, 4 and 6, $V_S = 100$ m/s), supporting a structural mass located at $H_c = 20$ m and subjected to ten acceleration time histories, all registered during real earthquakes. For sake of simplicity, we considered the above accelerations as free field

surface accelerations ($\ddot{u}_{ff0}$), that is we ignored any stratigraphic amplification effects. Table 3 summarizes the values of peak acceleration, *PGA*, duration, $T_{5–95}$ and mean frequency, f_m. Figure 9 shows (a) the acceleration time histories and (b) the Fourier amplitude spectra, while Fig. 10 shows the elastic response spectra at 5 % damping of the ten signals.

Figure 11 shows, for earthquake No. 7 and for $B/H = 1$ and 4: (a, b) the acceleration time histories and (c) the elastic response spectrum at 5 % damping of both free-field motion and FIM, the latter computed according to methods M1 and M2. As expected, filtering effects depend strongly on the ratio B/H, with a maximum reduction of about 50 % in the horizontal peak acceleration computed for $B/H = 1$, together with the appearance of a significant rocking component. Looking at the response spectra of Fig. 11c, the combined effect of translation and rotation of the foundation turns out to be either beneficial or detrimental for the structural system, depending on the ratio B/H, the major effects arising in the short period range. For the case at hand ($H_c = 20$ m), procedure M1 provides a maximum amplification in the spectral ordinates of 65 % for $B/H = 1$ and a maximum reduction of 40 % for $B/H = 4$, with respect to the free-field condition. By comparing the results from methods M1 and M2, no substantial difference is observed in terms of maximum accelerations, the only difference being a phase shift in the time history. Moreover, neglecting phase angles in the computation of the FIM introduces only small errors in the spectral ordinates, with a maximum value of 25 % for structural periods larger than 0.2 s ($B/H = 4$), always on the conservative side. These observations apply to all the earthquakes considered in this work.

Figure 12 shows, for all earthquakes and for $B/H = 1$, 4 and 6, the ratio of FIM to free-field response spectral ordinates, the former computed according to methods M1 and M2. The figure shows also the values $|I_u| + |I_\theta| \cdot H_c/H$ (method M3), and those of $|I_u|$, to highlight errors in reducing the design spectrum of the free-field motion without taking into account $|I_\theta|$. Depending on the ratio B/H, i.e. on the interplay between the reduction in the horizontal motion and the introduction of rocking oscillations, kinematic interaction may lead to either an increase ($B/H = 1$) or a reduction ($B/H = 4$, 6) of the spectral ordinates, with respect to the free-field case. Both simplified procedures M2 and M3 allow to take into account these effects, providing always conservative results with respect to the rigorous procedure M1. However, the error introduced reduces with increasing periods, where the foundation rocking tends to vanish and, for $T > 0.2$ s—i.e. for most of the real structures where considering the filtering effect induced by the foundation embedment makes sense—the maximum error associated to methods M2 and M3 is 35 and 40 % respectively. On the

Table 3 Ground motion parameters of input earthquakes

#	Earthquake	PGA (g)	$T_{5–95}$ (s)	f_m (Hz)
1	Kocaeli—Turkey (1999)	0.34	17.6	2.67
2	Loma Prieta—USA (1989)	0.37	15.7	4.11
3	Friuli—Italy (1976)	0.32	4.8	3.98
4	Imperial Valley—USA (1979)	0.33	10.3	4.34
5	Hollister—USA (1961)	0.19	9.2	2.84
6	Kobe—Japan (1995)	0.33	18.6	4.11
7	Trinidad—USA (1983)	0.17	3.2	4.30
8	Northridge—USA (1983)	0.58	19.0	3.38
9	Chi Chi—Taiwan (1999)	0.21	9.4	4.23
10	Landers—USA (1992)	0.44	22.3	5.72

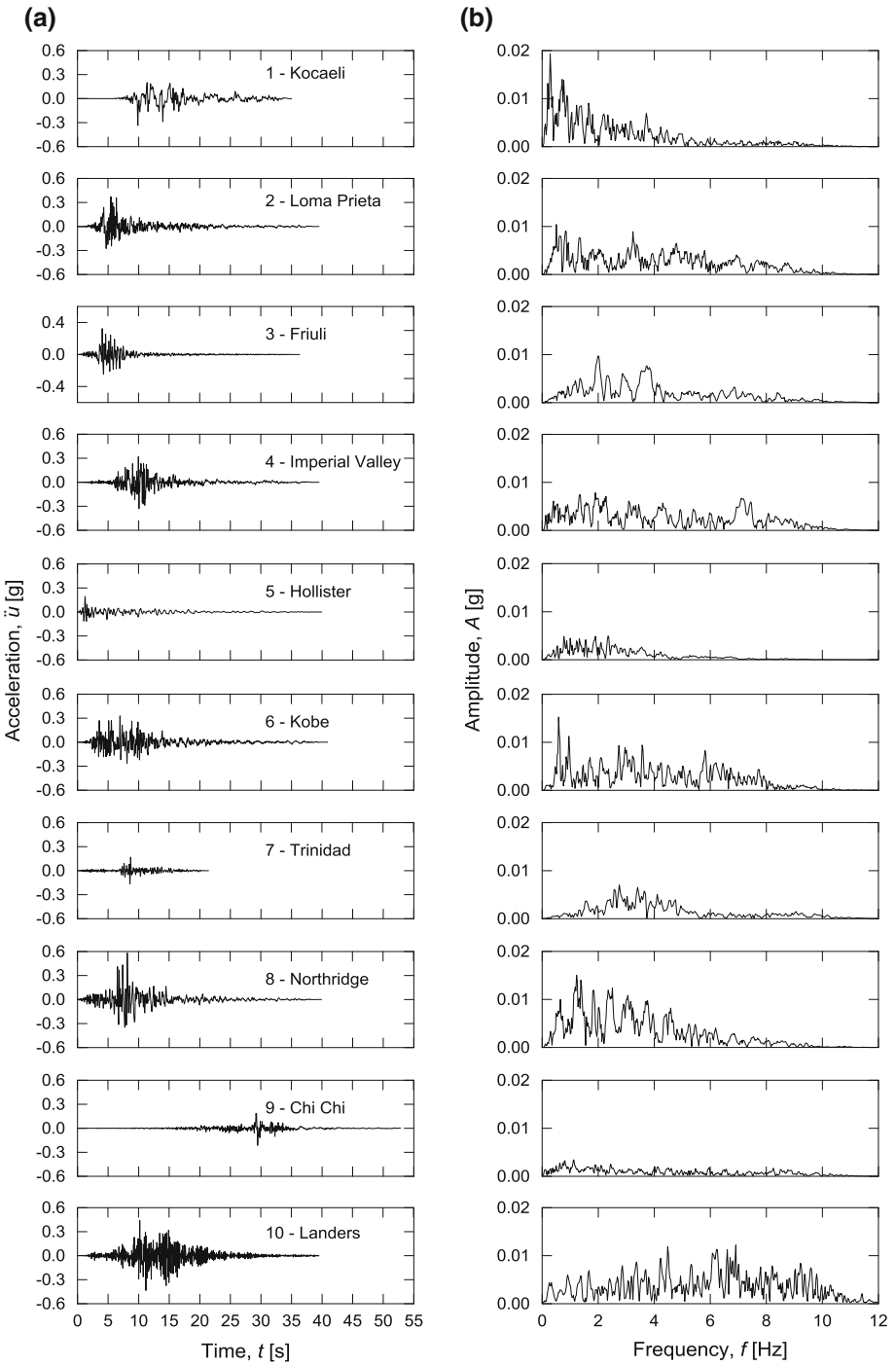

Fig. 9 Ten real earthquakes: **a** acceleration time histories and **b** Fourier amplitude spectra

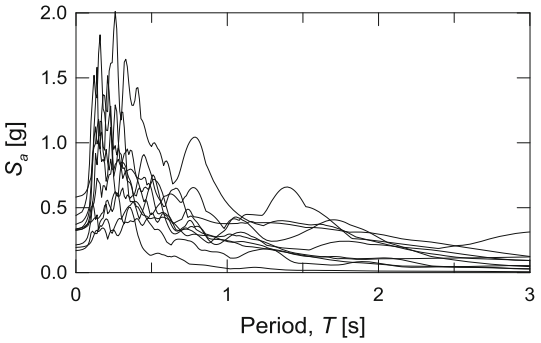

Fig. 10 Ten real earthquakes: elastic response spectra

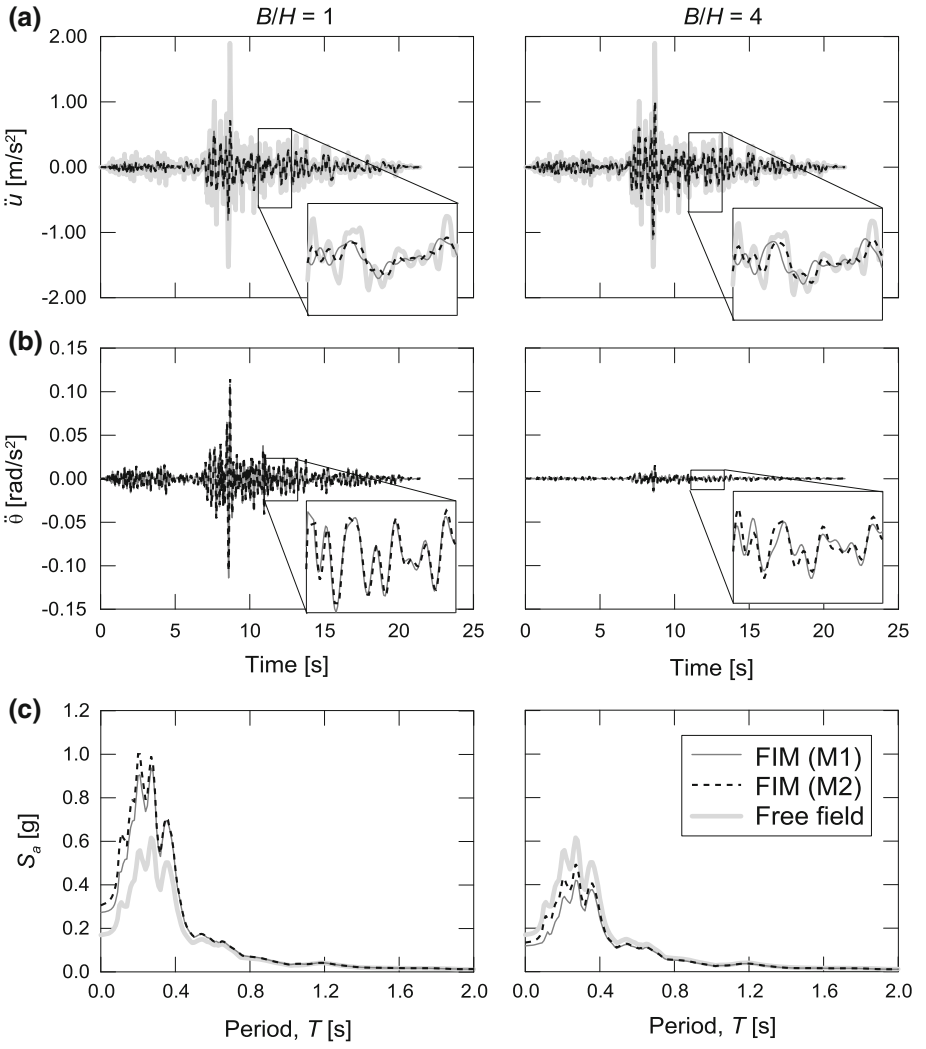

Fig. 11 Earthquake No. 7—acceleration time histories of: **a** horizontal translation and **b** rocking of free-field motion and FIM, together with **c** their elastic response spectra

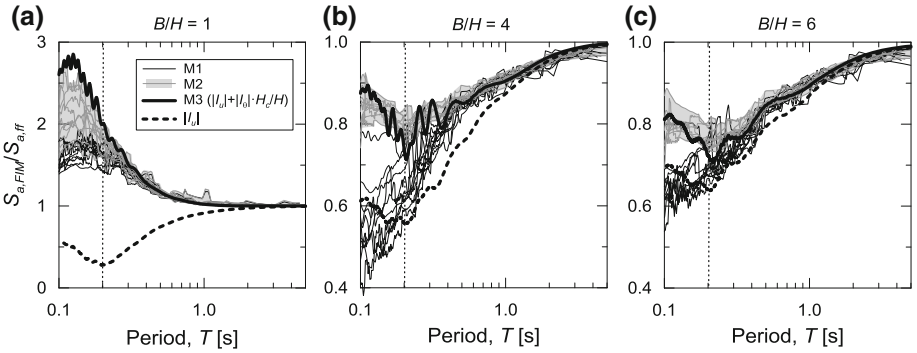

Fig. 12 All earthquakes: ratio of the response spectra between FIM and free-field motion for: **a** $B/H = 1$, **b** $B/H = 4$ and **c** $B/H = 6$ ($H = 6$ m, $H_c = 20$ m, $V_S = 100$ m/s)

other hand, in spite of being always unconservative, using solely $|I_u|$ provides a reasonable approximation of the actual trend for large values of B/H ($B/H \geq 4$), where the foundation rocking is small.

Based on the above observations, it can be concluded that both procedures M2 and M3 can be adopted effectively in the design practice, when computing the design motion either as a time history or as an elastic response spectrum, to take into account in a simplified manner filtering effects induced by embedded foundations.

6 Conclusions

This work was devoted to the filtering effects induced by rigid massless embedded foundations subjected to vertically propagating shear waves. Based on results from dimensional analysis and numerical simulations, it was found that the problem can be reasonably described solely by two dimensionless groups, namely: (1) $\omega H/V_S$, relating the wave length of the signal to the embedment depth of the foundation, and (2) the aspect ratio of the foundation, B/H, where B is the foundation width in the polarization plane.

New simplified and physically sound expressions were derived for the kinematic interaction factors, $|I_u|$ and $|I_\theta|$, and standard methods for using these functions in the evaluation of the FIM were critically reviewed, with reference to both static and dynamic procedures for the seismic design of structures. More in detail, it was pointed out that real-valued functions $|I_u|$ and $|I_\theta|$ can be used instead of complex-valued factors I_u and I_θ. Moreover, filtering functions can be applied either to the Fourier amplitude spectrum or to the response spectrum of the free-field signal, if the design motion must be specified as a time history or acceleration spectrum respectively.

In order to reduce the problem, usual approximations of linear viscoelastic material and uniform half-space were assumed for the soil. Possible nonlinearities or non-uniformities, leading to variability of shear wave velocity with induced strain level or depth, could be taken into account using conventional procedures, as summarized in Brandenberg et al. (2015). At one hand, non-uniform soil profiles could be introduced by using the time-averaged shear wave velocity (depth/travel time) for the soil included within the embedment depth of the foundation. On the other hand, when dealing with strong earthquakes, corresponding to which the induced shear strains can lead to a significant reduction of the

mobilised shear modulus of the soil, a site-specific ground response analysis should be performed to obtain values of strain-compatible shear modulus (and associated equivalent-linear V_s). Following Idriss and Sun (1993), the computed peak shear strain (γ_{max}) must be converted to a representative uniform strain ($\gamma_{eff} = \alpha \cdot \gamma_{max}$), where $\alpha = (M - 1)/10$ and M is the moment magnitude of the earthquake. Then, γ_{eff} is used to compute the mobilised shear modulus from the selected modulus reduction curve for the soil.

However, this equivalent-linear procedure does not allow to take into account the occurrence of plastic phenomena within the soil–foundation system, such as the formation of gaps between the foundation and the soil, slippage along the side walls and yielding of the soil itself at specific locations around the foundation (Gazetas 2015). Further studies are needed to explore these phenomena, all possibly affecting the dynamic behaviour of embedded foundations and, hence, also their filtering action on the signal transmitted to the structure.

The results of this work could be extended to explore the role of the stiffness of the foundation in cases where the rigidity assumption is no longer applicable, and to examine other realistic foundation layouts combining features of piled and embedded foundations.

Acknowledgments The work presented in this paper was developed with the financial support of the Italian Department of Civil Protection within the ReLUIS research project.

Appendix

Coefficients a_1, a_2, a_3, a_4 in Eqs. (8) and (9) are computed as a function B/H from the best fit of numerical data:

$$a_1(B/H) = \frac{(B/H)^{\alpha}}{\beta + (B/H)^{\alpha}} \quad \alpha = 1.04 \quad \beta = 4.24 \tag{11}$$

$$a_2(B/H) = \frac{\alpha + (B/H)}{1 + (B/H)} \quad \alpha = 1.92 \tag{12}$$

$$a_3(B/H) = \frac{1}{1 + \sqrt{B/H}} + \alpha(B/H)^{\beta} \quad \alpha = 0.32 \quad \beta = 0.38 \tag{13}$$

$$a_4(B/H) = \frac{1}{1 + \alpha(B/H)^{\beta}} \quad \alpha = 1.70 \quad \beta = 1.62 \tag{14}$$

References

Avilés J, Suarez M, Sanchez-Sesma FJ (2002) Effects of wave passage on the relevant dynamic properties of structures with flexible foundation. Earthqu Eng Struct Dyn 31:139–159

Bielak J (1975) Dynamic behavior of structures with embedded foundations. Earthqu Eng Struct Dyn 3:259–274

Brandenberg SJ, Mylonakis G, Stewart J (2015) Kinematic framework for evaluating seismic earth pressures on retaining walls. J Geotech Geoenviron Eng 141(7):04015031

Day SM (1978) Seismic response of embedded foundations. In: Proceedings of the ASCE convention, Chicago, Preprint No. 3450

Di Laora R, de Sanctis L (2013) Piles-induced filtering effect on the foundation input motion. Soil Dyn Earthq Eng 46:52–63
Dominguez J (1978) Response of embedded foundations to travelling waves. Report R78-24, Department of Civil Engineering, Massachusetts Institute of Technology, Cambridge
Elsabee F, Morray JP (1977) Dynamic behavior of embedded foundation. Rep. No. R77-33, Department of Civil Engineering, Massachusetts Institute of Technology, Cambridge
FEMA 440 (2005) Improvement of nonlinear static seismic analysis procedures. Federal Emergency Management Agency, Washington
Gazetas G (2015) 4th Ishihara lecture: soil–foundation–structure systems beyond conventional seismic failure thresholds. Soil Dyn Earthq Eng 68:23–39
Idriss IM, Sun JI (1993) User's manual for SHAKE91. Center for Geotechnical Modeling, Dept. of Civil and Environmental Engineering, University of California, Davis
Itasca (2011) FLAC fast Lagrangian analysis of continua v.7.0. User's manual
Joyner WB, Chen ATF (1975) Calculation of nonlinear ground response in earthquakes. Bull Seismol Soc Am 65:1315–1336
Karabalis DL, Beskos DE (1986) Dynamic response of 3-D embedded foundations by the boundary element method. Comput Methods Appl Mech Eng 56:91–119
Kim S, Stewart J (2003) Kinematic soil–structure interaction from strong motion recordings. J Geotech Geoenviron Eng 129(4):323–335
Luco JE, Wong HL (1987) Seismic response of foundations embedded in a layered half-space. Earthqu Eng Struct Dyn 15:233–247
Mahsuli M, Ghannad MA (2009) The effect of foundation embedment on inelastic response of structures. Earthq Eng Struct Dyn 38(4):423–437
Mita A, Luco JE (1989) Impedance functions and input motions for embedded square foundations. J Geotech Eng ASCE 115:491–503
Mylonakis G, Gazetas G (2000) Seismic soil–structure interaction: beneficial or detrimental? J Earthq Eng 4(3):277–301
Mylonakis G, Nikolaou S, Gazetas G (2006) Footings under seismic loading: analysis and design issues with emphasis on bridge foundations. Soil Dyn Earthq Eng 26(9):824–853
Politopoulos I (2010) Response of seismically isolated structures to rocking type excitations. Earthqu Eng Struct Dyn 39:325–342
Politopoulos I, Sergis I, Wang F (2015) Floor response spectra of a partially embedded seismically isolated nuclear plant. Soil Dyn Earthq Eng 78:213–217
Rayhani MHT, El Naggar MH (2008) Numerical modeling of seismic response of rigid foundation on soft soil. Int J Geomech 8:336–346
Stewart JP (2000) Variations between foundation-level and free-field earthquake ground motions. Earthqu Spectra 16:511–532
Vega J, Aznárez JJ, Santana A, Alarcón E, Padrón LA, Pérez JJ, Maeso O (2013) On soil–structure interaction in large non-slender partially buried structures. Bull Earthq Eng 11:1403–1421
Veletsos AS, Prasad AM, Wu WH (1997) Transfer functions for rigid rectangular foundations. Earthqu Eng Struct Dyn 26:5–17